JOURNAL OF VIROLOGY, May 2006, p. 4673–4682 Vol. 80, No. 10
0022-538X/06/$08.00+0 doi:10.1128/JVI.80.10.4673–4682.2006

Monomeric APOBEC3G Is Catalytically Active and Has Antiviral Activity

Sandrine Opi,[1] Hiroaki Takeuchi,[1] Sandra Kao,[1] Mohammad A. Khan,[1] Eri Miyagi,[1] Ritu Goila-Gaur,[1] Yasumasa Iwatani,[2] Judith G. Levin,[2] and Klaus Strebel[1]*

Laboratory of Molecular Microbiology, Viral Biochemistry Section, National Institute of Allergy and Infectious Diseases, National Institutes of Health, Building 4, Room 310, 4 Center Drive, MSC 0460, Bethesda, Maryland 20892-0460,[1] and Laboratory of Molecular Genetics, National Institute of Child Health and Human Development, National Institutes of Health, Bethesda, Maryland 20892[2]

Received 18 October 2005/Accepted 18 February 2006

APOBEC3G (APO3G) is a cytidine deaminase that restricts replication of *vif*-defective human immunodeficiency virus type 1 (HIV-1). Like other members of the cellular deaminase family, APO3G has the propensity to form homo-multimers. In the current study, we investigated the functional determinants for multimerization of human APO3G and studied the role of APO3G multimerization for catalytic activity, virus encapsidation, and antiviral activity. We found that human APO3G is capable of forming multimeric complexes in transfected HeLa cells. Interestingly, multimerization of APO3G was exquisitely sensitive to RNase treatment, suggesting that interaction of APO3G subunits is facilitated or stabilized by an RNA bridge. Mutation of a conserved cysteine residue (C97) that is part of an N-terminal zinc-finger motif in APO3G abolished multimerization of APO3G; however, the C97 mutation inhibited neither in vitro deaminase activity nor antiviral function of APO3G. These results suggest that monomeric APO3G is both catalytically active and has antiviral activity. Interference studies employing either catalytically inactive or packaging-incompetent APO3G variants suggest that wild-type APO3G is packaged into HIV-1 particles in monomeric form. These results provide novel insights into the catalytic function and antiviral property of APO3G and demonstrate an important role for C97 in the RNA-dependent multimerization of this protein.

APOBEC3G (APO3G) belongs to a family of cytidine deaminases that in humans includes APOBEC1, APOBEC2, eight APOBEC3 variants designated APOBEC3A through -3H, and APOBEC4, as well as activation-induced deaminase (7, 12, 30, 40). The activity of APO3G interferes with the replication of a broad range of retroviruses and can also block hepatitis B virus (39), whose replication cycle involves the reverse transcription of a pregenomic RNA intermediate (33). Interestingly, human immunodeficiency virus type 1 (HIV-1) Vif can counteract the antiviral activity of APO3G by inhibiting its incorporation into virions (13, 24, 34, 36). This inhibition is at least in part due to a reduction in cellular APO3G expression, which has been attributed primarily to Vif-mediated degradation of APO3G by cytoplasmic proteasomes (6, 19, 24, 25, 34, 36, 44).

It is now well established that packaging of APO3G into virus particles can result in hypermutation of the viral minus-strand cDNA during reverse transcription (10, 17, 22, 23, 43, 45). Interestingly, human APO3G is not only packaged into human immunodeficiency viruses but is also incorporated into simian immunodeficiency viruses and murine leukemia virus (10, 22, 23). The efficient packaging of APO3G into such diverse viruses could suggest that the mechanism of APO3G packaging is either relatively nonspecific or requires signals shared by these viruses. The observation that deletions in various regions of APO3G can prevent packaging into virus particles (4, 18) argues in favor of a specific packaging mechanism.

* Corresponding author. Mailing address: NIH, NIAID, 4/312, 4 Center Drive, MSC 0460, Bethesda, MD 20892-0460. Phone: (301) 496-3132. Fax: (301) 402-0226. E-mail: kstrebel@nih.gov.

APO3G binds to RNA in vitro, a property that it shares with other members of the APOBEC family of proteins (3, 12, 21). Indeed, even though some studies concluded that viral RNA was not essential for encapsidation of APO3G (2, 4, 9, 20, 27, 37), the packaging efficiency was clearly enhanced by the presence of viral or nonviral RNA (15, 20, 32, 37). Furthermore, we found that APO3G packaged nonspecifically into HIV-1 particles in the absence of viral RNA lacked stable association with the viral core; in contrast, the presence of viral RNA promoted the stable association of APO3G with the viral reverse transcription complex (15). Aside from binding to RNA, packaging of APO3G may further require an interaction with the viral Gag precursor. This is suggested by the fact that deletions in Gag, in particular NC, abolished the packaging of APO3G into virus-like particles (2, 20, 32, 37).

APO3G has the propensity to form multimers (12, 16, 27, 35, 41). However, the functional significance of APO3G multimerization has thus far remained unexplored. In this study we investigated the role of APO3G multimerization for catalytic activity, virus encapsidation, and antiviral activity. We found that APO3G multimerization was sensitive to RNase treatment, suggesting an involvement of viral or cellular RNA in this process. Interestingly, multimerization was also exquisitely sensitive to mutation of a single cysteine residue (C97) in an N-terminal zinc-finger domain, while mutation of a second cysteine in the same domain (C100) or mutation of two cysteine residues in a C-terminal zinc-finger domain (C288 or C291) had no effect on multimerization. Interestingly, encapsidation of APO3G was sensitive to mutation of C100, while mutation of C97, C288, and C291 did not inhibit APO3G packaging. However, mutation of C288 and C291 completely abrogated APO3G deaminase activity. Remarkably, mutation of C97 did not inhibit the deaminase

activity of virus-associated APO3G. These results suggest that APO3G enzymatic activity is independent of multimerization. Finally, APO3G antiviral activity also does not require multimerization and is not absolutely dependent on catalytic activity; however, catalytically active APO3G is more effective in inhibiting HIV-1 replication.

MATERIALS AND METHODS

Plasmids. The *vif*-defective molecular clone pNL4-3ΔVif (14) was used for the production of virus stocks. Construction of pcDNA-APO3G:MycHis for the expression of C-terminally epitope-tagged wild-type human APO3G was reported elsewhere (13). Stop codons were introduced into the pcDNA-APO3G-MycHis vector by PCR-based mutagenesis for the expression of untagged human APO3G proteins. For simplicity, we refer to vectors expressing MycHis-tagged APO3G as pcDNA-APO3G:MycHis and use the designation pcDNA-APO3G when referring to authentic untagged human APO3G. Proteins are referred to as APO3G-myc (C-terminally MycHis-tagged APO3G) and APO3G (untagged protein), respectively. Mutation of cysteine residues C97, C100, C288, and C291 in human APO3G either alone or in combination was accomplished by PCR-based mutagenesis of pcDNA-APO3G. PCR products were cloned into pcDNA-APO3G or pcDNA-APO3G:MycHis to obtain pcDNA-APO3G C97A, pcDNA-APO3G C97A/C100L, pcDNA-APO3G C97A/C100S, pcDNA-APO3G C97A/C100A, pcDNA-APO3G C100S:MycHis, and pcDNA-APO3G C288S/C291A. The presence of the desired mutations and the absence of additional mutations were verified for each construct by sequence analysis.

Antisera. APO3G was identified using a polyclonal rabbit serum against recombinant human APO3G (13). For immunoprecipitation of APO3G, a myc-specific rabbit polyclonal antibody was used (Sigma-Aldrich, Inc., St. Louis, MO). Serum from an HIV-positive patient (APS) was used to detect HIV-1-specific capsid (CA) proteins.

Tissue culture and transfections. HeLa cells were propagated in Dulbecco's modified Eagle's medium containing 10% fetal bovine serum. For transfection, HeLa cells were grown in 25-cm^2 flasks to about 80% confluence. Cells were transfected using LipofectAMINE PLUS (Invitrogen Corp., Carlsbad, CA) following the manufacturer's recommendations. A total of 5 to 6 μg of plasmid DNA per 25-cm^3 flask (5×10^6 cells) was used unless indicated otherwise in the figure legends. Cells were harvested 24 to 48 h posttransfection.

Preparation of virus stocks. Virus stocks were prepared by transfecting HeLa cells with appropriate plasmid DNAs. Virus-containing supernatants were harvested 24 to 48 h after transfection. Cellular debris was removed by centrifugation (3 min, 3,000 × *g*), and clarified supernatants were filtered (0.45 μm) to remove residual cellular contaminants. For determination of viral infectivity, unconcentrated filtered viral supernatants were used for the infection of LuSIV indicator cells. For immunoblot analysis of viral proteins, virus-containing supernatants (7 ml) were concentrated by ultracentrifugation through 4 ml of 20% sucrose in phosphate-buffered saline (PBS) as described previously (13).

Infectivity assay. To determine viral infectivity, virus stocks were normalized for equal levels of reverse transcriptase activity and used to infect LuSIV cells (5×10^5) in a 24-well plate in a total volume of 1.2 to 1.4 ml. LuSIV cells are derived from CEMx174 cells and contain a luciferase indicator gene under the control of the SIVmac239 long terminal repeat (31). These cells were obtained through the NIH AIDS Research and Reference Reagent Program and were maintained in complete RPMI 1640 medium supplemented with 10% fetal bovine serum and hygromycin B (300 μg/ml). Cells were infected for 24 h at 37°C. Cells were then harvested and lysed in 150 μl of Promega 1× reporter lysis buffer (Promega Corp., Madison, WI). To determine the luciferase activity in the lysates, 50 μl of each lysate was combined with luciferase substrate (Promega Corp., Madison, WI) by automatic injection, and light emission was measured for 10 seconds at room temperature in a luminometer (Optocomp II; MGM Instruments, Hamden, CT).

Immunoblotting. For immunoblot analysis of intracellular proteins, whole-cell lysates were prepared as follows. Cells were washed once with PBS, suspended in PBS (400 μl/10^7 cells), and mixed with an equal volume of sample buffer (4% sodium dodecyl sulfate [SDS], 125 mM Tris-HCl, pH 6.8, 10% 2-mercaptoethanol, 10% glycerol, and 0.002% bromphenol blue). Proteins were solubilized by boiling for 10 to 15 min at 95°C with occasional vortexing of the samples to shear chromosomal DNA. Residual insoluble material was removed by centrifugation (2 min, 15,000 rpm in an Eppendorf Minifuge). For immunoblot analysis of virus-associated proteins, concentrated viral pellets were suspended in a 1:1 mixture of PBS and sample buffer and boiled. Cell lysates and viral extracts were subjected to SDS-polyacrylamide gel electrophoresis; proteins were transferred to polyvinylidene difluoride membranes and reacted with appropriate antibodies as described below. Membranes were then incubated with horseradish peroxidase-conjugated secondary antibodies (Amersham Biosciences, Piscataway, NJ) and visualized by enhanced chemiluminescence (Amersham Biosciences).

Immunoprecipitation analysis. For immunoprecipitation analysis of intracellular proteins, cell lysates were prepared as follows. Cells were washed once with PBS and lysed in 300 μl of lysis buffer (50 mM Tris, pH 7.5, 150 mM NaCl, 0.5% Triton X-100). The cell extracts were centrifuged at 13,000 × *g* for 3 min, and the supernatant was incubated on a rotating wheel for 1 h at 4°C with protein A-Sepharose (Sigma) coupled with anti-myc rabbit polyclonal antibody (Sigma). Immune complexes were washed three times with 50 mM Tris, 300 mM NaCl, and 0.1% Triton X-100 (pH 7.4). Bound proteins were eluted from beads by heating in sample buffer for 5 min at 96°C and analyzed by immunoblotting. For RNase treatment, cells were lysed in lysis buffer supplemented with 50 μg/ml of RNase A. The cell extracts were then subjected to immunoprecipitation as described above.

Deamination assay. For the analysis of virus-associated deaminase activity, virus-containing supernatants (7 ml) were precleared by filtration (0.45 μm) and pelleted through 20% sucrose (4 ml). Concentrated virions were directly suspended in 100 μl of deaminase buffer (40 mM Tris, pH 8.0, 40 mM KCl, 50 mM NaCl, 5 mM EDTA, 1 mM dithiothreitol, 2% [vol/vol] glycerol, and 0.1% [vol/vol] Triton X-100) and incubated with a 5′-^{32}P-end-labeled oligonucleotide substrate (5′-ATTATTATTA TTATTCCCAA TTATTTATTT ATTTATTTAT TT-3′ [23]) containing two potential APO3G target sites (underlined). After overnight incubation at 37°C with occasional agitation, the oligonucleotides were purified on G25 Quick Spin columns (Roche) and reacted with uracil-DNA glycosylase (Roche) for 2 h at 37°C in uracil-DNA glycosylase buffer (60 mM Tris-HCl, pH 8.0, 1 mM EDTA, 1 mM dithiothreitol, 0.001% bovine serum albumin) to remove the uracil bases generated by deamination. To cleave at the abasic site, the samples were treated for 5 min at 37°C with 0.15 M NaOH. Samples were then neutralized by the addition of 0.15 M HCl. The cleaved products were separated on 15% acrylamide–7 M urea gels and detected by autoradiography. Cleavage efficiency under these conditions was directly proportional to the amount of APO3G packaged into virions.

RESULTS

Multimerization of APO3G is sensitive to RNase treatment. To study multimerization of human APO3G, we coexpressed two forms of human APO3G, the authentic 384-amino-acid APO3G protein and a 409-residue variant carrying a C-terminal MycHis epitope tag. Multimerization of human APO3G was identified by the coimmunoprecipitation of the untagged protein when the corresponding tagged variant was precipitated with a myc-specific antibody. To test the ability of APO3G to form homo-multimers, HeLa cells were transfected with equal amounts of plasmids encoding untagged (APO3G) or myc epitope-tagged (APO3G-myc) APO3G proteins (Fig. 1). Mock-transfected cells were analyzed in parallel (Fig. 1, lanes 1 and 4). Cells were harvested 24 h posttransfection and lysed in lysis buffer. To control for protein expression, a portion of the lysates was analyzed directly by immunoblotting with an APO3G-specific antibody (Fig. 1, lanes 1 to 3). The remaining fraction of the lysates was first subjected to immunoprecipitation with a myc-specific polyclonal antibody and then analyzed by immunoblotting (Fig. 1, lanes 4 to 6). As can be seen, untagged and tagged APO3G were expressed at comparable levels (lane 2), and untagged APO3G was efficiently coimmunoprecipitated (lane 5) by its epitope-tagged analog. These results demonstrate that human APO3G forms homo-multimers in transfected HeLa cells.

APO3G is an RNA binding protein (12, 18, 27; Y. Iwatani et al., unpublished data), and the interaction of APO3G with viral RNA was previously shown to be required for the efficient packaging of APO3G into HIV-1 virions (15, 37). Furthermore, APO3G was found in RNase-sensitive high-molecular-mass com-

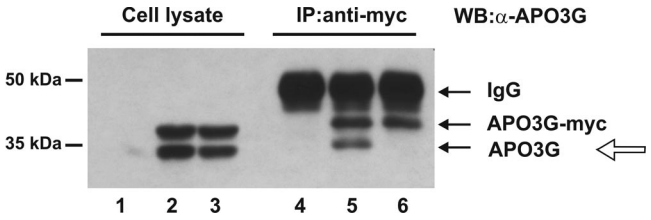

FIG. 1. APO3G multimerization is RNase sensitive. HeLa cells were cotransfected with equal amounts of plasmids expressing either untagged (APO3G) or MycHis epitope-tagged (APO3G-myc) human APO3G. After 24 h, cells were lysed in the absence (lanes 1, 2, 4, and 5) or presence (lanes 3 and 6) of 50 μg/ml RNase A. Samples were either directly analyzed (lanes 1 to 3) or immunoprecipitated with a myc-specific polyclonal antibody (lanes 4 to 6). Cell lysates and immunoprecipitates were analyzed by immunoblotting using an APO3G-specific rabbit polyclonal antibody followed by incubation with a horseradish peroxidase-conjugated anti-rabbit antibody. Proteins are identified on the right. In the immunoprecipitated samples, the horseradish peroxidase-conjugated antibody reacted both with the APO3G-specific antibodies and the myc-specific antibody used for the immunoprecipitation (immunoglobulin G [IgG]). The open arrow marks coimmunoprecipitated APO3G. IP, immunoprecipitation; WB, Western blot.

plexes (5). To test the possible role of RNA in the multimerization of APO3G, coimmunoprecipitation analysis of untagged and tagged APO3G was performed on RNase-treated samples. For this purpose cells were lysed in lysis buffer containing RNase A (50 μg/ml). Samples were either analyzed directly (Fig. 1, lane 3) or following immunoprecipitation with the Myc-specific antibody (Fig. 1, lane 6). As in the untreated samples, tagged and untagged APO3G proteins were expressed at similar levels (Fig. 1, compare lanes 2 and 3); however, RNase treatment abolished the coimmunoprecipitation of the untagged APO3G (lane 6). These results demonstrate that the formation of APO3G multimers is facilitated or stabilized by an RNA bridge.

Cysteine 97 is critical for multimerization of human APO3G. APO3G contains two potential zinc-coordinating motifs referred to here as N- and C-terminal zinc-finger domains, with the consensus sequence H-X-E-X_{23-28}-P-C-X_{2-4}-C (where X stands for any amino acid). To determine if these motifs play a role in APO3G multimerization, we generated a series of human APO3G mutants carrying substitutions in one or more of the four cysteine residues present in the N-terminal (C97 and C100) or C-terminal (C288 and C291) zinc-finger domains (Fig. 2A). HeLa cells were cotransfected with equimolar ratios of plasmids expressing tagged wild-type human APO3G (APO3G-myc) and untagged human APO3G mutants C97A, C97A/C100L, and C288S/C291A (Fig. 2B, lanes 3 to 5). Mock-transfected cells (Fig. 2B, lane 1) served as a negative control. A sample containing wild-type tagged and untagged APO3G was included as a positive control (Fig. 2B, lane 2). Total protein expression was analyzed by immunoblotting using an APO3G-specific antibody (Fig. 2B, top

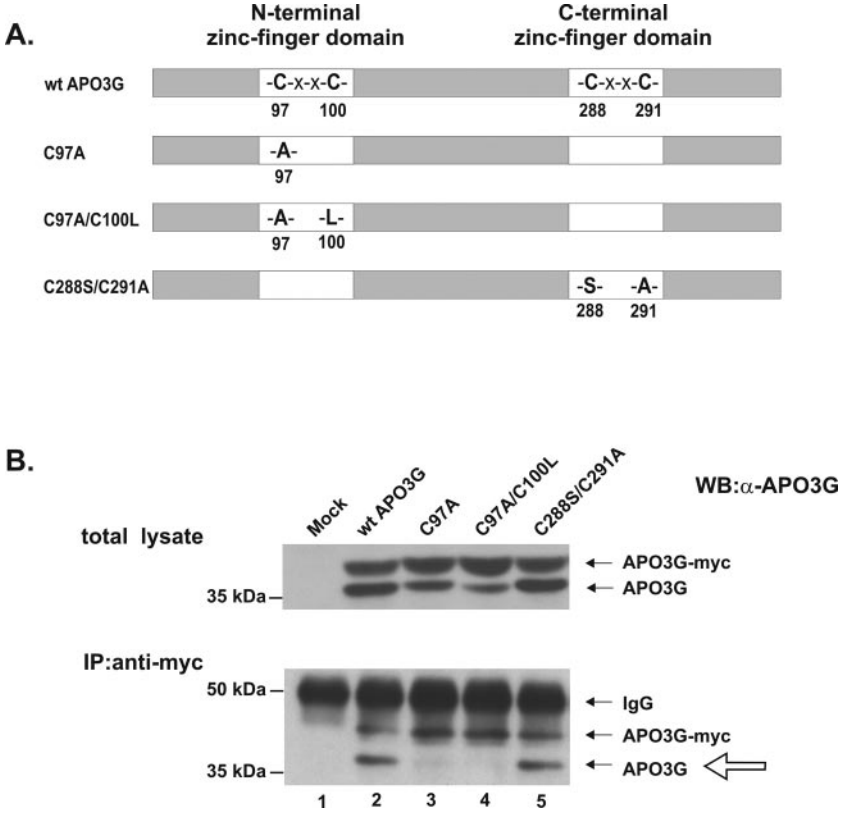

FIG. 2. C97 is important for multimerization of human APO3G. (A) Schematic representation of human APO3G zinc-finger domain mutants. (B) HeLa cells were cotransfected at equimolar ratios with vectors expressing tagged wild-type human APO3G and untagged variants of either wild-type APO3G (lane 2), C97A (lane 3), C97A/C100L (lane 4), or C288S/C291A (lane 5) APO3G mutants. Lane 1 is a mock-transfected control. After 24 h, cell lysates were subjected to immunoblotting either directly (total lysate) or following immunoprecipitation with a myc-specific antibody (lower panel) as described for Fig. 1. The open arrow marks the position of coimmunoprecipitated proteins.

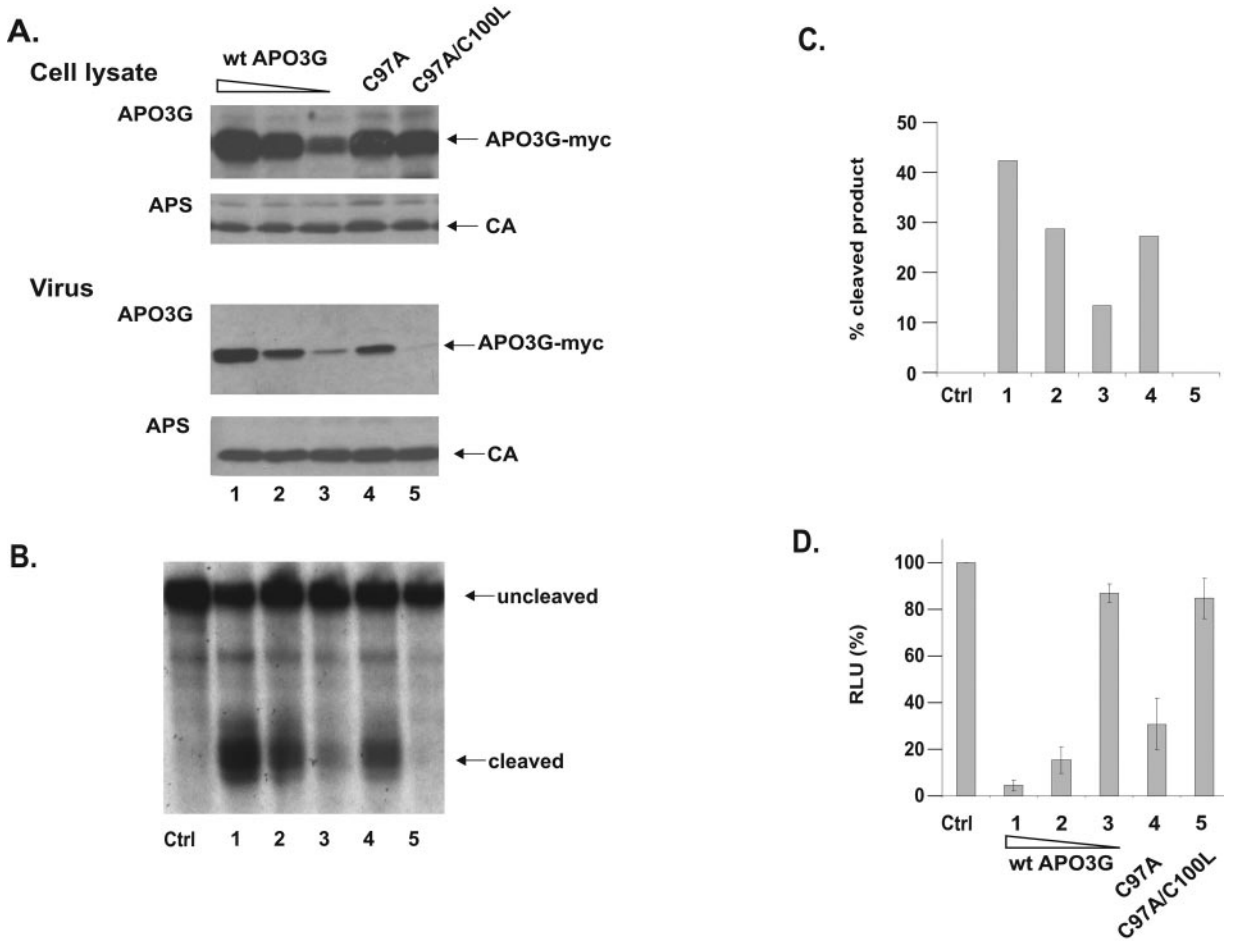

FIG. 3. Monomeric APO3G is catalytically active and has antiviral activity. *vif*-defective NL4-3 (4 μg) and various amounts of tagged wild-type APO3G-myc (lane 1, 2 μg; lane 2, 0.5 μg; lane 3, 0.125 μg) or APO3G C97A (lane 4, 2 μg) or C97A/C100L (lane 5, 2 μg) were cotransfected into HeLa cells. Total DNA amounts were adjusted to 6 μg in each sample using pcDNA3.1(-) vector DNA. (A) Cell lysates and virus-containing supernatants were collected 48 h after transfection and analyzed by immunoblotting using an APO3G-specific antibody (APO3G). The same blots were subsequently reprobed with an HIV-positive patient serum (APS). Proteins are identified on the right. CA, capsid protein. (B) Concentrated virus from the samples shown in panel A was used for an in vitro deamination assay using a 5′-^{32}P-end-labeled single-stranded DNA substrate as described in Materials and Methods. Cleaved and uncleaved oligonucleotides were separated by 15% acrylamide–7 M urea gel electrophoresis. The substrate contains two potential APO3G target sites resulting in two distinct cleavage products. (C) Cleaved and uncleaved products from panel B were quantified by PhosphorImager analysis. Deamination efficiency was expressed as the percentage of cleaved product (percentage of the combined cleaved and uncleaved samples). (D) Unconcentrated virus-containing supernatants from panel A were normalized for equivalent amounts of reverse transcriptase activity and used to determine the effect of APO3G mutations on antiviral activity in a single-cycle infectivity assay as described in Materials and Methods. Luciferase activity induced in infected LuSIV cells was determined 24 h after infection. Activity observed in cells infected with control virus produced in the absence of APO3G was defined as 100% (Ctrl). The infectivity of the other viruses was calculated relative to the control virus. Error bars are standard deviations from three independent infections.

panel). To assess the ability of APO3G mutants to interact with wild-type protein, cell lysates were immunoprecipitated with a myc-specific polyclonal antibody (bottom panel). As expected, untagged wild-type APO3G efficiently interacted with tagged wild-type APO3G (lane 2). Similarly, mutation of the two cysteine residues in the C-terminal zinc-finger domain (C288S and C291A) (lane 5) did not affect the ability of the mutant protein to multimerize with wild-type APO3G. In contrast, mutants containing a mutation in C97 of the N-terminal zinc-finger domain, i.e., C97A (lane 3) and C97A/C100L (lane 4), were unable to interact with wild-type APO3G. Changing C100 to serine or alanine in the context of the C97A mutation (C97A/C100S and C97A/C100A) similarly abolished the ability of the mutant proteins to interact with wild-type APO3G (data not shown). However, mutation of C100 alone did not interfere with APO3G multimerization (see Fig. 4A, lane 6, below). These results suggest that C97 plays a critical role in the multimerization of human APO3G.

Monomeric APO3G is catalytically active and has antiviral activity. Having demonstrated the importance of C97 in APO3G for multimerization, we next investigated the importance of multimerization for the packaging of APO3G into HIV-1 particles. HeLa cells were transfected with *vif*-deficient NL4-3 and mutant APO3G plasmids. To control for protein expression, cell lysates and concentrated cell-free virus preparations were analyzed 48 h later by immunoblotting using an APO3G-specific antibody (Fig. 3A, APO3G) or an HIV-positive human patient serum (Fig. 3A, APS). Wild-type APO3G was efficiently packaged into HIV-1 particles in a dose-dependent manner (Fig. 3A, lanes 1 to 3).

Similarly, mutation of C97 in the N-terminal zinc-finger domain did not have a significant impact on the packaging of the mutant protein (Fig. 3A, lane 4). In contrast, mutation of both cysteine residues in the first zinc-finger domain severely reduced the packaging efficiency (Fig. 3A, lane 5). Similar results were observed for C97A/C100A and C97A/C100S mutants of APO3G (data not shown). These results demonstrate that the N-terminal zinc-finger domain is important for the packaging of APO3G into HIV-1 virions; however, multimerization does not appear to be a crucial requirement for APO3G encapsidation.

To determine the effect of mutations in the N-terminal zinc-finger domain for catalytic activity of APO3G, concentrated virus stocks derived from the same experiment shown in Fig. 3A were used for an in vitro deaminase assay as described in Materials and Methods. As expected, wild-type APO3G induced deamination of the substrate DNA in a dose-dependent manner (Fig. 3B, lanes 1 to 3). Remarkably, APO3G C97A also exhibited significant deaminase activity (Fig. 3B, lane 4). Indeed, by quantifying the data shown in Fig. 3B by PhosphorImager analysis and taking into account the relative amounts of virus-associated wild-type and mutant APO3G (Fig. 3A, compare virus lanes 2 and 4), we estimate that catalytic activity of the C97A APO3G mutant is close to that of the wild-type enzyme (Fig. 3C, compare lanes 2 and 4). These data suggest that, unlike APOBEC1 (29), multimerization of APO3G is not required for catalytic deaminase activity. Viruses produced in the presence of APO3G C97A/C100L did not exhibit detectable deaminase activity (Fig. 3B, lane 5). This is likely due to the fact that packaging of the double mutant is severely restricted (Fig. 3A, lane 5 of the virus samples).

To determine the antiviral activity of the APO3G mutants, culture supernatants from the experiment shown in Fig. 3A were used to infect LuSIV indicator cells, and virus infectivity was determined as described in Materials and Methods. The infectivity of virus produced in the absence of APO3G was defined as 100% (Fig. 3D, Ctrl). As expected, wild-type APO3G inhibited viral infectivity in a dose-dependent manner (Fig. 3D, lanes 1 to 3). Mutation of both cysteines in the N-terminal zinc-finger motif (C97A and C100L) almost completely abolished the APO3G antiviral activity (Fig. 3D, lane 5), presumably because of the inefficient packaging of the double mutant. Mutation of C97 on the other hand only moderately reduced the antiviral activity of the mutant APO3G, which retained a level of antiviral activity similar to that of the wild-type enzyme (Fig. 3D, compare lanes 2 and 4). From these experiments we conclude that monomeric APO3G not only has full catalytic activity, but also largely retains its antiviral function.

APO3G is packaged into HIV-1 particles as a monomer. A previous analysis of APOBEC1 found that, similar to our results on APO3G, mutation of C93 (which corresponds to C97 in APO3G) affected dimerization of the protein (26). Mutation of C96, on the other hand (corresponding to C100 in APO3G), had no effect on APOBEC1 dimerization. To test the role of C100 for the multimerization of APO3G, we performed coimmunoprecipitation studies of wild-type APO3G and an APO3G C100S mutant similar to those shown in Fig. 1 and 2. HeLa cells were transfected to express similar levels of untagged wild-type APO3G and either wild-type tagged APO3G (Fig. 4A, lane 2) or tagged APO3G C100S (Fig. 4A, lane 3). Mock-transfected cells were included as a control (lanes 1 and 4). Untagged wild-type

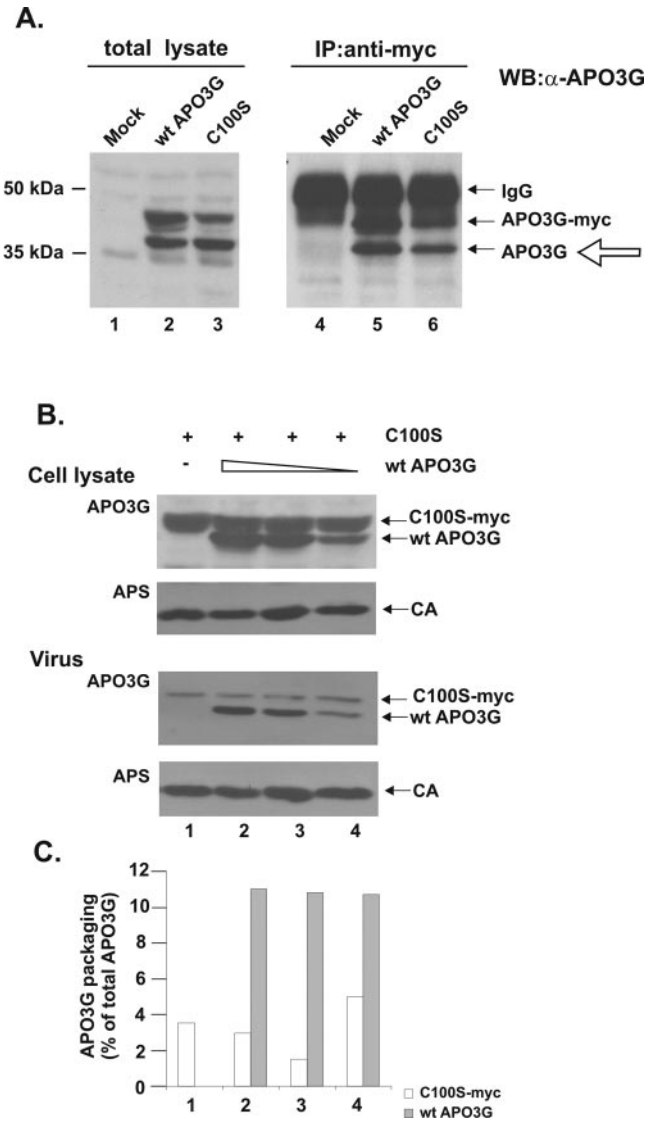

FIG. 4. Wild-type APO3G is packaged into HIV-1 particles as a monomer. (A) HeLa cells were mock transfected (lanes 1 and 4) or transfected with a combination of 1 μg of untagged wild-type pcDNA-APO3G and either 1 μg of tagged wild-type pcDNA-APO3G-myc (lanes 2 and 5) or 3 μg of tagged pcDNA-APO3G-C100S-myc (lanes 3 and 6). Different plasmid amounts were used to achieve comparable protein expression for wild-type and mutant proteins. Cells were harvested 24 h after transfection. Cell lysates were either directly analyzed by immunoblotting (lanes 1 to 3) or subjected first to immunoprecipitation with a myc-specific polyclonal antibody followed by immunoblotting using an APO3G-specific polyclonal antibody (lanes 4 to 6). Proteins are identified on the right. Coimmunoprecipitated proteins are marked by the open arrow. The secondary antibody used to recognize the polyclonal APO3G antibody also cross-reacted with the myc-specific antibody used for the immunoprecipitation (immunoglobulin G). (B) Constant amounts (3 μg) of tagged APO3G C100S and various amounts (1, 0.5, and 0.25 μg) of untagged wild-type human APO3G were cotransfected into HeLa cells together with *vif*-defective pNL4-3 vector DNA (2 μg). Empty pcDNA3.1(-) vector DNA was used to adjust total transfected DNA to 6 μg. Cells and virus-containing supernatants were analyzed 48 h after transfection by immunoblotting as described for Fig. 3A. (C) Packaging efficiency of wild-type APO3G and C100S was determined by quantifying the cellular and virus-associated protein shown in panel B. Signals were adjusted for loading volumes (cell lysate was 3.75% of total sample; virus was 15% of total sample), and the amount of protein in virus was calculated as a percentage of the total available intra- and extracellular pool. Open bars, APO3G C100S-myc; solid bars, wild-type APO3G.

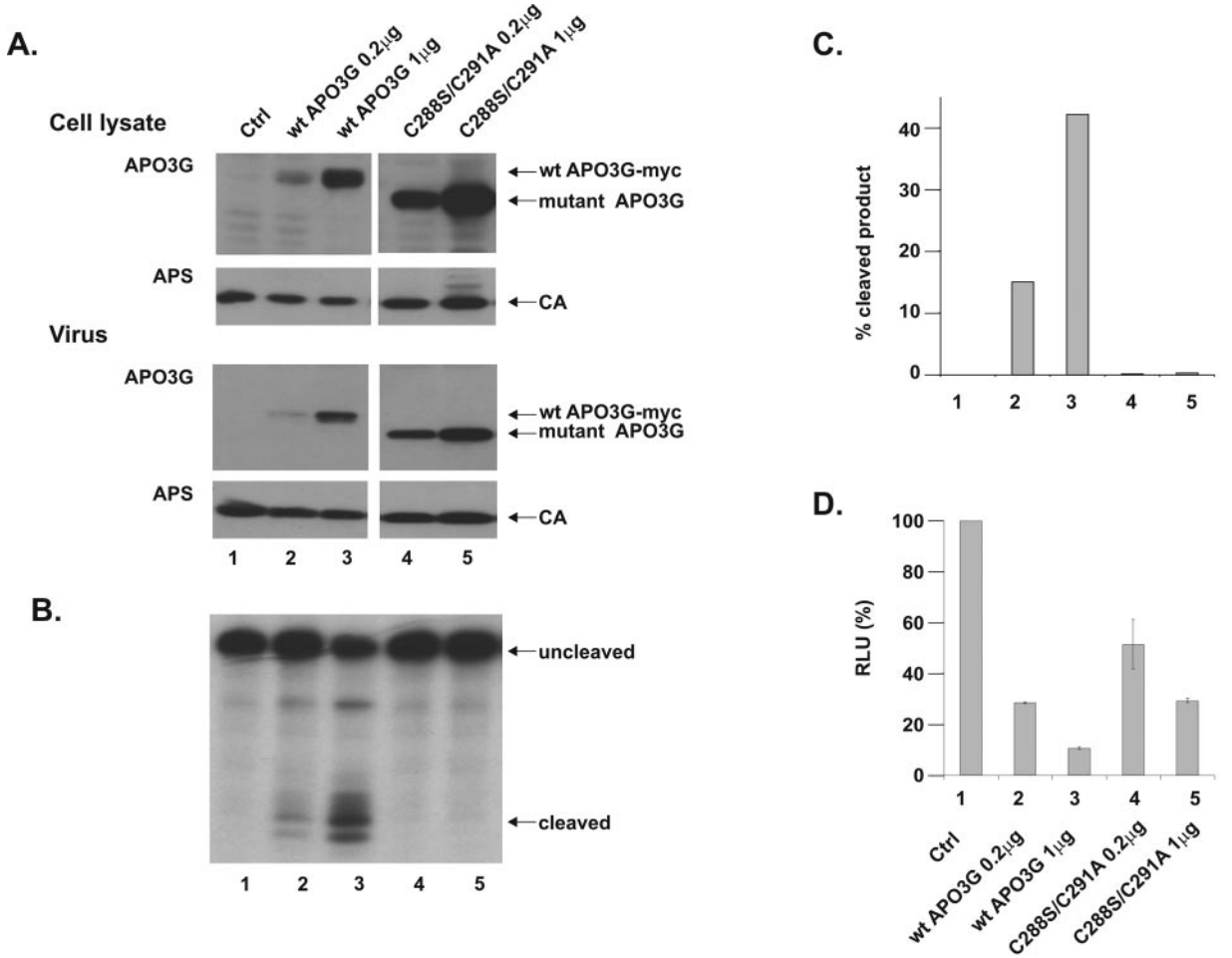

FIG. 5. APO3G deaminase activity is not absolutely required for antiviral activity. HeLa cells were cotransfected with *vif*-defective pNL4-3 vector DNA (4 μg) and 0.2 μg or 1 μg of vectors expressing tagged wild-type human APO3G (lanes 2 and 3) or untagged mutant APO3G C288S/C291A (lanes 4 and 5). Lane 1 is a control transfection of *vif*-defective NL4-3 vector without APO3G. (A) Cell lysates and virus-containing supernatants were analyzed using an APO3G-specific antibody (top panels). The same blots were subsequently reprobed with an HIV-positive patient serum (lower panels). Proteins are identified on the right. (B) Virus-associated deaminase activity was determined in an in vitro assay using a 5′-^{32}P-end-labeled single-stranded DNA substrate as described for Fig. 3B. (C) Cleaved and uncleaved products from panel B were quantified by PhosphorImager analysis. Deamination efficiency was expressed as the percentage of cleaved product (percentage of the combined cleaved and uncleaved samples). (D) Cell-free virus-containing supernatants were used to infect LuSIV indicator cells to determine viral infectivity as described in Materials and Methods. The relative infectivity of the virus stocks was determined 24 h after infection of the indicator cells. Luciferase values obtained for virus produced in the absence of APO3G were defined as 100%. Error bars are standard deviations from three independent infections.

APO3G was coimmunoprecipitated by tagged wild-type APO3G and tagged APO3G C100S with similar efficiency (Fig. 4A, compare lanes 5 and 6), suggesting that mutation of C100 does not affect the ability of APO3G to form hetero-multimeric complexes with wild-type APO3G. These results are therefore consistent with results from APOBEC1 studies and indicate that C97 but not C100 is critical for APO3G multimerization.

To determine the role of C100 in the packaging of APO3G, APO3G C100S was expressed in the presence of *vif*-defective NL4-3. HeLa cells were transfected with 2 μg of pNL4-3 DNA together with 3 μg of pcDNA-APO3G C100S-Myc DNA. Cell lysates and concentrated viral supernatants were subjected to immunoblot analysis as described for Fig. 3. We found that the APO3G C100S mutant was efficiently expressed in transfected cells but was packaged less efficiently than the wild-type protein (Fig. 4B and C, lane 1). These results suggest that cysteine 100 in the N-terminal zinc-finger domain is not essential for APO3G multimerization but is required for the efficient packaging of the protein into HIV-1 particles.

To further investigate the role of multimerization for APO3G packaging into HIV-1 particles, we measured the packaging efficiency of the multimerization-competent (but packaging-impaired) APO3G C100S mutant in the presence of increasing amounts of wild-type APO3G. As shown in Fig. 4B, expression of increasing amounts of wild-type APO3G in the presence of constant levels of APO3G C100S had no influence on the packaging of the C100S mutant, which remained low even in the presence of high levels of wild-type APO3G (Fig. 4B and C, compare lanes 2 to 4). Conversely, expression of APO3G C100S did not affect the packaging efficiency of wild-type APO3G, which remained constant at all levels of expression (Fig. 4C). Because of the efficient hetero-multimerization

of wild-type and C100S APO3G (Fig. 4A, lane 6), the lack of cooperative packaging of APO3G C100S and the lack of interference with the packaging of wild-type protein by mutant APO3G both suggest that wild-type APO3G is packaged in the monomeric form.

Deaminase-defective APO3G retains partial antiviral activity. It was previously shown that the catalytic activity of APOBEC-1 can be inhibited in a dominant-negative fashion through the formation of heterodimeric complexes with a catalytically inactive mutant (29). If APO3G dimerization or multimerization were important for catalytic activity, we would predict a similar dominant-negative effect for catalytically inactive but multimerization-competent APO3G variants. A possible candidate for a dominant-negative mutant of APO3G is the C-terminal zinc-finger mutant C288S/C291A, which we found to efficiently multimerize with wild-type APO3G (Fig. 2B, lane 5). Our first goal was to verify that this mutant was efficiently packaged into HIV-1 particles but was catalytically inactive. HeLa cells were transfected with DNA encoding *vif*-defective pNL4-3 together with two concentrations (0.2 or 1 μg) of DNA expressing tagged wild-type APO3G or untagged APO3G C288S/C291A. To control for protein expression, cell lysates and concentrated cell-free virus preparations were analyzed 48 h later by immunoblotting using an APO3G-specific antibody (Fig. 5A, APO3G) or an HIV-positive human patient serum (Fig. 5A, APS). Both wild-type (Fig. 5A, lanes 2 and 3) and APO3G C288S/C291A (lanes 4 and 5) were packaged efficiently and in a dose-dependent manner into *vif*-defective HIV-1 particles.

Determination of APOBEC3G catalytic activity in an in vitro deaminase assay (see Materials and Methods) revealed a complete lack of catalytic activity in viruses containing APO3G C288S/C291A (Fig. 5B and C, lanes 4 and 5). In contrast, viruses containing wild-type APO3G exhibited significant deaminase activity, which was directly correlated to the amount of APO3G packaged into the virions (Fig. 5B and C, lanes 2 and 3). No deaminase activity was detected in viruses lacking APO3G (Fig. 5B and C, lane 1). Quantitation of the data from Fig. 5B demonstrated that at the highest concentration of wild-type APO3G, about 40% of the substrate was deaminated (Fig. 5C, lane 3) while deamination by the C288S/C291A C288S/C291A was undetectable (Fig. 5C, lane 5). These results are consistent with previous reports confirming the importance of the C-terminal zinc-finger domain for catalytic activity (27, 28, 35).

To correlate virus-associated deaminase activity with the antiviral effect of APO3G, the infectivity of the viruses analyzed in Fig. 5A and B was determined in a single-cycle infectivity assay (Fig. 5D) as described in Materials and Methods. Infectivity of *vif*-defective virus lacking APO3G was defined as 100% (Fig. 5D, lane 1) and used to calculate the relative infectivity of virus stocks containing various amounts of wild-type or mutant APO3G (Fig. 5D, lanes 2 to 5). As expected, packaging of increasing amounts of wild-type APO3G resulted in a dose-dependent reduction in viral infectivity (Fig. 5D, lanes 2 and 3). Surprisingly, packaging of deaminase-defective APO3G (lanes 4 and 5) also caused a significant and dose-dependent reduction in viral infectivity. However, taking into account the overall higher amounts of virus-associated mutant APO3G in this experiment relative to wild-type APO3G (Fig. 5A, virus, compare lanes 2 and 3 with lanes 4 and 5), the antiviral effect of wild-type APO3G is significantly stronger than that of the deaminase-defective mutant. In conclusion, we verified that the APO3G C288S/C291A mutant is packaged with wild-type efficiency into HIV-1 particles and is indeed catalytically inactive, yet retains some antiviral activity.

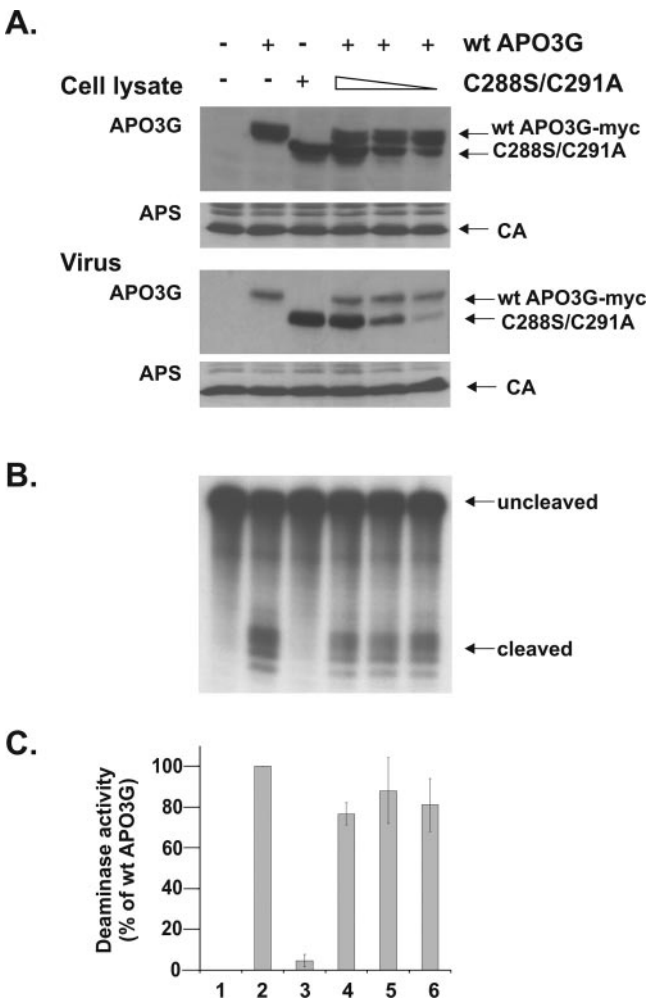

FIG. 6. Catalytically inactive APO3G does not competitively inhibit wild-type APO3G deaminase activity. HeLa cells were transfected with constant amounts of tagged wild-type APO3G (wt APO3G-myc) and various amounts of untagged APO3G C288S/C291A (lanes 4 to 6). Lane 1 is a control transfection of the NL4-3 vector without APO3G. Wild-type APO3G (lane 2) and APO3G C288S/C291A (lane 3) were expressed individually as positive and negative controls, respectively. (A) Cell lysates and virus-containing supernatants were collected 48 h after transfection and subjected to immunoblotting as described for Fig. 3. (B) Virus-associated deaminase activity was determined as described for Fig. 3B. A representative gel from three independent experiments is shown. (C) Quantitation was performed as described for Fig. 3B, except that the deaminase activity of wild-type APO3G in the absence of mutant APO3G C288S/C291A (lane 2) was defined as 100%. Error bars reflect the standard deviation calculated from three independent experiments.

Catalytically inactive but multimerization-competent APO3G C288S/C291A fails to competitively inhibit the deaminase activity of wild-type APO3G. We next tested the possible dominant-negative effect of APO3G C288S/C291A on wild-type APO3G. HeLa cells were transfected with constant amounts of tagged wild-type APO3G and/or varying amounts of untagged

APO3G C288S/C291A mutant (Fig. 6). Protein expression and virus production were controlled by immunoblotting as described for Fig. 3. As expected, wild-type and mutant APO3G proteins were efficiently expressed and packaged into Vif-deficient HIV-1 particles in a dose-dependent manner (Fig. 6A). Importantly, expression of increasing amounts of APO3G C288S/C291A did not affect the packaging of wild-type APO3G, demonstrating the absence of a competitive packaging mechanism and verifying that overall APO3G expression remained at subsaturating levels.

Analysis of virus-associated deaminase activity (Fig. 6B) was performed as described for Fig. 3B and revealed robust activity in the sample containing only wild-type APO3G (Fig. 6B, lane 2), which was defined as 100% (Fig. 6C, lane 2). In samples containing only mutant APO3G (Fig. 6B, lane 3), no catalytic deaminase activity was detectable despite the presence of high levels of mutant APO3G in the virus preparations. Coexpression of increasing amounts of mutant APO3G with constant amounts of wild-type APO3G (Fig. 6B, lanes 4 to 6) did not reveal a dominant-negative effect of APO3G C288S/C291A on the catalytic activity of wild-type APO3G. The quantitation of the deaminase activity is shown in Fig. 6C and represents the average of three independent experiments. There was a moderate reduction of deaminase activity in some of the samples coexpressing mutant APO3G. However, the effect of APO3G C288S/C291A is not dose dependent and therefore most likely reflects experimental variation rather than true functional interference. Taken together, these results further suggest that APO3G monomers have deaminase activity. Our data do not completely rule out the possibility that hetero-multimers of APO3G containing one functional C-terminal zinc-finger domain are catalytically active. Such a possibility, however, seems unlikely, since in such a scenario, coexpression of mutant APO3G should increase the overall deaminase activity, as both wild-type APO3G homo-multimers and wild-type–mutant hetero-multimers would be catalytically active. This effect was not observed (Fig. 6C, compare lanes 4 to 6). Thus, our results are best explained by a model in which APO3G acts as a monomer.

DISCUSSION

APO3G is a member of a larger family of cytidine deaminases that can target either RNA or DNA substrates. All cytidine deaminases analyzed to date, including activation-induced deaminase, APOBEC1, APOBEC2, APOBEC3B, and APOBEC3G, were found to form homo-dimers or homo-multimers (8, 12, 16, 26, 27, 35, 38, 41). However, with the exception of APOBEC1, the role of multimerization for catalytic activity of these enzymes remains unclear (29). In this study we have investigated the role of APO3G multimerization on deaminase activity, incorporation into viral particles, and antiviral activity. Our data demonstrate for the first time that APO3G multimerization is not required for any of these functions. The lack of functional importance of APO3G multimerization contrasts with the observation that APOBEC1 dimerization is required for its editing activity (29). In the case of APOBEC1, a mutant form similar to our C288S/C291A mutant was still capable of forming dimers with the wild-type protein and inhibited the activity of wild-type APOBEC1 in a dominant-negative manner; however, catalytically inactive mutants that poorly dimerized failed to inhibit wild-type deaminase activity (29). Our experiments analyzing potential dominant-negative effects of a C-terminal zinc-finger domain mutant (C288S/C291A), which efficiently multimerized with wild-type APO3G and was packaged into HIV-1 particles but was enzymatically inactive, failed to show evidence for dominant-negative interference (Fig. 6). Similarly, the multimerization-competent C100S mutant that was packaged with reduced efficiency did not lower the packaging efficiency of coexpressed wild-type APO3G, nor did coexpression of wild-type APO3G increase the packaging efficiency of the C100S mutant (Fig. 4B). Finally, mutation of C97 in APO3G inhibited multimerization (Fig. 2) but did not affect enzymatic activity (Fig. 3B and C). The latter results are consistent with a previous report demonstrating enzymatic activity of a C97 APO3G mutant in a bacterial assay system (28). Remarkably, APO3G C97 was efficiently packaged into HIV-1 particles (Fig. 3A) and retained similar antiviral activity as wild-type APO3G (Fig. 3D). Based on the combined results from these experiments we conclude that (i) monomeric APO3G is packaged into HIV-1 particles, (ii) monomeric APO3G is catalytically active, and (iii) monomeric APO3G has antiviral activity.

Unlike APO3G, which has two zinc-finger motifs, APOBEC1 contains only a single catalytic domain (for a review, see reference 11). Molecular modeling based on the crystal structure of its yeast ortholog CDD1 predicted that the zinc-finger domain of each APOBEC1 monomer lines up on opposite faces of a head-to-head dimer (42). It is conceivable that the two zinc-finger domains of a single APO3G monomer align such that they form a catalytically active pocket similar to that formed by the APOBEC1 dimer. Future structural analyses are needed to test such a model. Nevertheless, it is clear from these data that the two zinc-finger domains in APO3G are not functionally equivalent. The N-terminal zinc-finger domain is responsible for RNA binding, multimerization, and virus incorporation, while APO3G enzymatic activity resides in the C-terminal zinc-finger motif (our data and Iwatani et al., unpublished data) (27, 28, 35, 45).

It is unclear why mutation of C97 and C100 in human APO3G differentially impacted protein multimerization and virus incorporation. Our data clearly demonstrate that APO3G multimerization is RNase sensitive and thus likely to be mediated or stabilized by an RNA bridge (Fig. 1). It is therefore conceivable that mutation of C97 affects RNA binding by APO3G. This would be consistent with results from APOBEC1 studies, where mutation of C93 (corresponding to C97 in APO3G) was found to greatly reduce its RNA binding in vitro (21). On the other hand, APO3G C97A was efficiently packaged into HIV-1 virions, a property that we previously found to be RNA dependent (15). In the same vein, lack of RNA binding by APO3G C100 could explain the inefficient virion incorporation but would not account for its ability to multimerize. Thus, a mere change in the RNA binding properties of the C97 and C100 mutants does not satisfactorily explain the differential activities of these mutants. We have investigated the possibility that C97 contributes to APO3G multimerization through formation of disulfide-linked dimers. However, analysis of APO3G under nonreducing conditions did not reveal any evidence for the existence of such disulfide-linked dimers (data not shown). Thus, while our data clearly define a role of C97 in the

multimerization of APO3G, future studies will have to address the precise mechanism of multimerization.

A recent study by Chiu and coworkers reported on the identification of a novel, postentry restriction by APO3G to HIV-1 replication (5). The authors found that expression of APO3G in a low-molecular-mass form correlated with high resistance to HIV-1 infection in resting $CD4^+$ cells. Activation of $CD4^+$ cells resulted in a shift of APO3G to an enzymatically inactive RNase-sensitive high-molecular-mass complex that no longer provided protection from HIV-1 infection (5). The inability of APO3G C97A to multimerize predicts that this mutant lost its ability to assemble into high-molecular-mass complexes. It will therefore be interesting to investigate whether APO3G C97A has constitutive antiviral activity that is active on a postentry level and is Vif independent, as would be expected based on the results of Chiu et al.

It is also interesting that even though mutation of the C-terminal zinc-finger motif in APO3G resulted in the loss of enzymatic activity, the mutant proteins retained significant antiviral activity, though not as much as the wild-type protein (Fig. 5). These findings contrast with those of a previous report that found that mutation of the C-terminal zinc-finger motif eliminated the catalytic activity of APO3G but had virtually no effect on its antiviral activity (28). We do not currently understand the reason for the antiviral property of catalytically inactive APO3G; however, it is conceivable that it is associated with the high-level expression and efficient packaging of the C288S/C291A mutant in our experiment. In that regard, we would like to point to our previous observation that even Vif protein, which is normally critical for the production of infectious viruses, can have strong antiviral activity when expressed at high levels in virus-producing cells (1). This antiviral effect of Vif is independent of APO3G and is caused by the binding of virus-associated Vif to Gag precursor molecules, which in turn affects proteolytic processing of Gag and induces a maturation defect that interferes with the infectivity of the affected virions (1). Thus, careful titration experiments will be required to determine if the antiviral effect of catalytically inactive APO3G is specific or, as in the case of Vif, simply reflects an overexpression phenomenon.

ACKNOWLEDGMENTS

We are grateful to Alicia Buckler-White, Ron Plishka, and Christopher Erb for oligonucleotide synthesis and sequence analysis. We thank Jason Roos and Janice Clements for the LuSIV indicator cell line. The latter was obtained through the NIH Research and Reference Reagent Program.

This work was supported in part by a grant from the NIH Intramural AIDS Targeted Antiviral Program to K.S. and by the Intramural Research Program of the NIH, NIAID, and NICHD.

REFERENCES

1. **Akari, H., M. Fujita, S. Kao, M. A. Khan, M. Shehu-Xhilaga, A. Adachi, and K. Strebel.** 2004. High level expression of human immunodeficiency virus type-1 Vif inhibits viral infectivity by modulating proteolytic processing of the Gag precursor at the p2/nucleocapsid processing site. J. Biol. Chem. **279:**12355–12362.
2. **Alce, T. M., and W. Popik.** 2004. APOBEC3G is incorporated into virus-like particles by a direct interaction with HIV-1 Gag nucleocapsid protein. J. Biol. Chem. **279:**34083–34086.
3. **Anant, S., A. J. MacGinnitie, and N. O. Davidson.** 1995. APOBEC-1, the catalytic subunit of the mammalian apolipoprotein B mRNA editing enzyme, is a novel RNA-binding protein. J. Biol. Chem. **270:**14762–14767.
4. **Cen, S., F. Guo, M. Niu, J. Saadatmand, J. Deflassieux, and L. Kleiman.** 2004. The interaction between HIV-1 Gag and APOBEC3G. J. Biol. Chem. **279:**33177–33184.
5. **Chiu, Y. L., V. B. Soros, J. F. Kreisberg, K. Stopak, W. Yonemoto, and W. C. Greene.** 2005. Cellular APOBEC3G restricts HIV-1 infection in resting $CD4^+$ T cells. Nature **435:**108–114.
6. **Conticello, S. G., R. S. Harris, and M. S. Neuberger.** 2003. The Vif protein of HIV triggers degradation of the human antiretroviral DNA deaminase APOBEC3G. Curr. Biol. **13:**2009–2013.
7. **Conticello, S. G., C. J. Thomas, S. K. Petersen-Mahrt, and M. S. Neuberger.** 2005. Evolution of the AID/APOBEC family of polynucleotide (deoxy)cytidine deaminases. Mol. Biol. Evol. **22:**367–377.
8. **Dickerson, S. K., E. Market, E. Besmer, and F. N. Papavasiliou.** 2003. AID mediates hypermutation by deaminating single stranded DNA. J. Exp. Med. **197:**1291–1296.
9. **Douaisi, M., S. Dussart, M. Courcoul, G. Bessou, R. Vigne, and E. Decroly.** 2004. HIV-1 and MLV Gag proteins are sufficient to recruit APOBEC3G into virus-like particles. Biochem. Biophys. Res. Commun. **321:**566–573.
10. **Harris, R. S., K. N. Bishop, A. M. Sheehy, H. M. Craig, S. K. Petersen-Mahrt, I. N. Watt, M. S. Neuberger, and M. H. Malim.** 2003. DNA deamination mediates innate immunity to retroviral infection. Cell **113:**803–809.
11. **Harris, R. S., and M. T. Liddament.** 2004. Retroviral restriction by APOBEC proteins. Nat. Rev. Immunol. **4:**868–877.
12. **Jarmuz, A., A. Chester, J. Bayliss, J. Gisbourne, I. Dunham, J. Scott, and N. Navaratnam.** 2002. An anthropoid-specific locus of orphan C to U RNA-editing enzymes on chromosome 22. Genomics **79:**285–296.
13. **Kao, S., M. A. Khan, E. Miyagi, R. Plishka, A. Buckler-White, and K. Strebel.** 2003. The human immunodeficiency virus type 1 Vif protein reduces intracellular expression and inhibits packaging of APOBEC3G (CEM15), a cellular inhibitor of virus infectivity. J. Virol. **77:**11398–11407.
14. **Karczewski, M. K., and K. Strebel.** 1996. Cytoskeleton association and virion incorporation of the human immunodeficiency virus type 1 Vif protein. J. Virol. **70:**494–507.
15. **Khan, M. A., S. Kao, E. Miyagi, H. Takeuchi, R. Goila-Gaur, S. Opi, C. L. Gipson, T. G. Parslow, H. Ly, and K. Strebel.** 2005. Viral RNA is required for the association of APOBEC3G with human immunodeficiency virus type 1 nucleoprotein complexes. J. Virol. **79:**5870–5874.
16. **Lau, P. P., H. J. Zhu, A. Baldini, C. Charnsangavej, and L. Chan.** 1994. Dimeric structure of a human apolipoprotein B mRNA editing protein and cloning and chromosomal localization of its gene. Proc. Natl. Acad. Sci. USA **91:**8522–8526.
17. **Lecossier, D., F. Bouchonnet, F. Clavel, and A. J. Hance.** 2003. Hypermutation of HIV-1 DNA in the absence of the Vif protein. Science **300:**1112.
18. **Li, J., M. J. Potash, and D. J. Volsky.** 2004. Functional domains of APOBEC3G required for antiviral activity. J. Cell Biochem. **92:**560–572.
19. **Liu, B., X. Yu, K. Luo, Y. Yu, and X. F. Yu.** 2004. Influence of primate lentiviral Vif and proteasome inhibitors on human immunodeficiency virus type 1 virion packaging of APOBEC3G. J. Virol. **78:**2072–2081.
20. **Luo, K., B. Liu, Z. Xiao, Y. Yu, X. Yu, R. Gorelick, and X. F. Yu.** 2004. Amino-terminal region of the human immunodeficiency virus type 1 nucleocapsid is required for human APOBEC3G packaging. J. Virol. **78:**11841–11852.
21. **MacGinnitie, A. J., S. Anant, and N. O. Davidson.** 1995. Mutagenesis of APOBEC-1, the catalytic subunit of the mammalian apolipoprotein B mRNA editing enzyme, reveals distinct domains that mediate cytosine nucleoside deaminase, RNA binding, and RNA editing activity. J. Biol. Chem. **270:**14768–14775.
22. **Mangeat, B., P. Turelli, G. Caron, M. Friedli, L. Perrin, and D. Trono.** 2003. Broad antiretroviral defence by human APOBEC3G through lethal editing of nascent reverse transcripts. Nature **424:**99–103.
23. **Mariani, R., D. Chen, B. Schrofelbauer, F. Navarro, R. Konig, B. Bollman, C. Munk, H. Nymark-McMahon, and N. R. Landau.** 2003. Species-specific exclusion of APOBEC3G from HIV-1 virions by Vif. Cell **114:**21–31.
24. **Marin, M., K. M. Rose, S. L. Kozak, and D. Kabat.** 2003. HIV-1 Vif protein binds the editing enzyme APOBEC3G and induces its degradation. Nat. Med. **9:**1398–1403.
25. **Mehle, A., B. Strack, P. Ancuta, C. Zhang, M. McPike, and D. Gabuzda.** 2004. Vif overcomes the innate antiviral activity of APOBEC3G by promoting its degradation in the ubiquitin-proteasome pathway. J. Biol. Chem. **279:**7792–7798.
26. **Navaratnam, N., T. Fujino, J. Bayliss, A. Jarmuz, A. How, N. Richardson, A. Somasekaram, S. Bhattacharya, C. Carter, and J. Scott.** 1998. Escherichia coli cytidine deaminase provides a molecular model for ApoB RNA editing and a mechanism for RNA substrate recognition. J. Mol. Biol. **275:**695–714.
27. **Navarro, F., B. Bollman, H. Chen, R. Konig, Q. Yu, K. Chiles, and N. R. Landau.** 2005. Complementary function of the two catalytic domains of APOBEC3G. Virology **333:**374–386.
28. **Newman, E. N., R. K. Holmes, H. M. Craig, K. C. Klein, J. R. Lingappa, M. H. Malim, and A. M. Sheehy.** 2005. Antiviral function of APOBEC3G can be dissociated from cytidine deaminase activity. Curr. Biol. **15:**166–170.
29. **Oka, K., K. Kobayashi, M. Sullivan, J. Martinez, B. B. Teng, K. Ishimura-Oka, and L. Chan.** 1997. Tissue-specific inhibition of apolipoprotein B mRNA editing in the liver by adenovirus-mediated transfer of a dominant

negative mutant APOBEC-1 leads to increased low density lipoprotein in mice. J. Biol. Chem. **272:**1456–1460.

30. **Rogozin, I. B., M. K. Basu, I. K. Jordan, Y. I. Pavlov, and E. V. Koonin.** 2005. APOBEC4, a new member of the AID/APOBEC family of polynucleotide (deoxy)cytidine deaminases predicted by computational analysis. Cell Cycle **4:**1281–1285.
31. **Roos, J. W., M. F. Maughan, Z. Liao, J. E. Hildreth, and J. E. Clements.** 2000. LuSIV cells: a reporter cell line for the detection and quantitation of a single cycle of HIV and SIV replication. Virology **273:**307–315.
32. **Schafer, A., H. P. Bogerd, and B. R. Cullen.** 2004. Specific packaging of APOBEC3G into HIV-1 virions is mediated by the nucleocapsid domain of the gag polyprotein precursor. Virology **328:**163–168.
33. **Seeger, C., and W. S. Mason.** 2000. Hepatitis B virus biology. Microbiol. Mol. Biol. Rev. **64:**51–68.
34. **Sheehy, A. M., N. C. Gaddis, and M. H. Malim.** 2003. The antiretroviral enzyme APOBEC3G is degraded by the proteasome in response to HIV-1 Vif. Nat. Med. **9:**1404–1407.
35. **Shindo, K., A. Takaori-Kondo, M. Kobayashi, A. Abudu, K. Fukunaga, and T. Uchiyama.** 2003. The enzymatic activity of CEM15/APOBEC-3G is essential for the regulation of the infectivity of HIV-1 virion but not a sole determinant of its antiviral activity. J. Biol. Chem. **278:**44412–44416.
36. **Stopak, K., C. de Noronha, W. Yonemoto, and W. C. Greene.** 2003. HIV-1 Vif blocks the antiviral activity of APOBEC3G by impairing both its translation and intracellular stability. Mol. Cell **12:**591–601.
37. **Svarovskaia, E. S., H. Xu, J. L. Mbisa, R. Barr, R. J. Gorelick, A. Ono, E. O. Freed, W. S. Hu, and V. K. Pathak.** 2004. Human apolipoprotein B mRNA-editing enzyme-catalytic polypeptide-like 3G (APOBEC3G) is incorporated into HIV-1 virions through interactions with viral and nonviral RNAs. J. Biol. Chem. **279:**35822–35828.
38. **Ta, V. T., H. Nagaoka, N. Catalan, A. Durandy, A. Fischer, K. Imai, S. Nonoyama, J. Tashiro, M. Ikegawa, S. Ito, K. Kinoshita, M. Muramatsu, and T. Honjo.** 2003. AID mutant analyses indicate requirement for class-switch-specific cofactors. Nat. Immunol. **4:**843–848.
39. **Turelli, P., B. Mangeat, S. Jost, S. Vianin, and D. Trono.** 2004. Inhibition of hepatitis B virus replication by APOBEC3G. Science **303:**1829.
40. **Wedekind, J. E., G. S. Dance, M. P. Sowden, and H. C. Smith.** 2003. Messenger RNA editing in mammals: new members of the APOBEC family seeking roles in the family business. Trends Genet. **19:**207–216.
41. **Wiegand, H. L., B. P. Doehle, H. P. Bogerd, and B. R. Cullen.** 2004. A second human antiretroviral factor, APOBEC3F, is suppressed by the HIV-1 and HIV-2 Vif proteins. EMBO J. **23:**2451–2458.
42. **Xie, K., M. P. Sowden, G. S. Dance, A. T. Torelli, H. C. Smith, and J. E. Wedekind.** 2004. The structure of a yeast RNA-editing deaminase provides insight into the fold and function of activation-induced deaminase and APOBEC-1. Proc. Natl. Acad. Sci. USA **101:**8114–8119.
43. **Yu, Q., R. Konig, S. Pillai, K. Chiles, M. Kearney, S. Palmer, D. Richman, J. M. Coffin, and N. R. Landau.** 2004. Single-strand specificity of APOBEC3G accounts for minus-strand deamination of the HIV genome. Nat. Struct. Mol. Biol. **11:**435–442.
44. **Yu, X., Y. Yu, B. Liu, K. Luo, W. Kong, P. Mao, and X. F. Yu.** 2003. Induction of APOBEC3G ubiquitination and degradation by an HIV-1 Vif-Cul5-SCF complex. Science **302:**1056–1060.
45. **Zhang, H., B. Yang, R. J. Pomerantz, C. Zhang, S. C. Arunachalam, and L. Gao.** 2003. The cytidine deaminase CEM15 induces hypermutation in newly synthesized HIV-1 DNA. Nature **424:**94–98.